Modes of Interannual Tropical Ocean–Atmosphere Interaction—a Unified View. Part II: Analytical Results in the Weak-Coupling Limit

J. DAVID NEELIN AND FEI-FEI JIN*

Department of Atmospheric Sciences, University of California, Los Angeles, Los Angeles, California

(Manuscript received 24 December 1991, in final form 23 February 1993)

ABSTRACT

The properties of the eigenmodes of the coupled tropical ocean–atmosphere system, linearized about a climatological basic state—and hence of the first bifurcation, which strongly determines the nature of the interannual variability, such as El Niño—show considerable dependence on the parameters of the coupled system. These eigenmodes are examined in a modified shallow-water model with simplified mixed-layer dynamics and a sea surface temperature (SST) equation, coupled to a simple atmospheric model. The model is designed so as to make analytical approximations feasible in various limits, as in a previous study by Neelin where the x-periodic case was analyzed. The realistic case of a finite ocean basin is treated here. An integral formulation of the eigenvalue problem is derived that provides a basis for making consistent approximations that include the effects of atmospheric and oceanic boundary conditions. We provide a scaling analysis to select parameters that give the most succinct insights into the behavior of the system, and outline the portions of this parameter space that are accessible to analytic results through the limits explored here and in Part III of this study. Important limits include the *fast-wave limit*, the limit where the time scale of ocean adjustment is fast compared to the time scale of SST change by coupled processes, and its converse, the *fast-SST limit*. The region of validity of the *weak-coupling limit* overlaps both of these, while that of the *strong-coupling limit* overlaps the fast-SST limit and approaches the region of validity of the fast-wave limit without a formal matching region.

In this part, we examine the weak-coupling limit, in which one expects the modes to be most closely related to those of the uncoupled problem. Here we treat two classes of mode from the uncoupled case: the SST modes (related to the time derivative of the SST equation) and the discrete modes from the ocean-dynamics spectrum, the ocean basin modes. From the numerical results of Part I, we know that away from the weak-coupling and fast-wave limits, the continuous surfaces in parameter space formed by the eigenvalues of each type of mode are joined, so that through most of parameter space the coupled modes are best characterized as *mixed SST/ocean-dynamics modes*. Series solutions for the weakly coupled modes are found to have radii of convergence that extend over modest but significant ranges of coupling values. The transition from the uncoupled modes to the fundamentally coupled mixed modes is examined. For the SST modes, coupling effects come to dominate the structure of basin-scale modes even at tiny coupling values. The structure of the ocean basin modes persists over a perceptible range of coupling, but structure changes involving the SST equation enter importantly as coupling is increased and the transition to mixed-mode structure occurs at small coupling, well within the range of the weak-coupling limit. This suggests that intuition and terminology borrowed from the uncoupled system is of limited value in analyzing coupled models and that it is more productive to consider prototype modes in fully coupled regimes.

1. Introduction

Interactions between the tropical ocean and atmosphere produce interannual climate variability whose effects are felt globally (e.g., Rasmusson and Wallace 1983; Ropelewski and Halpert 1987; Pan and Oort 1991; Ghil and Vautard 1991), among which the El Niño–Southern Oscillation phenomenon has been the object of much interest (e.g., Bjerknes 1969; Wyrtki 1975; Rasmusson and Carpenter 1982; Gill and Rasmusson 1983; Cane 1986; Graham et al. 1987a,b; Lau and Sheu 1988; Deser and Wallace 1990; Rasmusson et al. 1990; Graham and White 1990; Philander 1990; Barnett 1991). The properties of the first bifurcation of the coupled tropical ocean–atmosphere system from the climate state largely determine the nature of the interannual variability (e.g., Neelin 1990; Münnich et al. 1991). A great deal about the behavior of the system may thus be understood in terms of the eigenmodes of the system, linearized about the climatological basic state. However, the sensitivity of the coupled system, both in relatively simple models (e.g., Philander et al. 1984; Cane and Zebiak 1985; Hirst 1988; Schopf and Suarez 1988, 1990; Battisti and Hirst 1989; Wakata and Sarachik 1991; Cane et al. 1990; Neelin 1991) and

* Current affiliation: Department of Meteorology, University of Hawaii at Manoa, Honolulu, Hawaii.

Corresponding author address: Prof. David Neelin, Dept. of Atmospheric Sciences, UCLA, 405 Hilgard Ave., Los Angeles, CA 90024-1565.

in coupled GCMs (e.g., as summarized in Neelin et al. 1992), has made the relation between the various flow regimes encountered challenging to understand. In Part I (Jin and Neelin 1993a) of this paper we examined the modes of the coupled system in a model closely related to the Zebiak and Cane (1987) model: a simple atmospheric model coupled to a modified shallow-water ocean with simplified mixed-layer dynamics and a sea surface temperature (SST) equation for an equatorial band, following Neelin (1991, N91 hereafter). We argued on the basis of numerical results that the connection between the various regions of parameter space for the coupled system could be understood in a straightforward manner.

The two basic ingredients of the coupled system that may be understood at low coupling are the oceanic dynamics modes [which in a closed basin are just the leaky basin modes of Cane and Moore (1981) and a class of scattering modes, as shown in appendix A] and the SST modes, which are related to the time derivative of the SST equation. These two kinds of modes are intrinsically separated (in the sense that the eigenvalue is determined by subsystems involving time derivatives associated with ocean dynamics or SST equations, respectively; eigenvectors of ocean-dynamics modes can have nonzero SST components, and vice versa) when the system is uncoupled or in the fast-wave limit (the limit where oceanic dynamics is in Sverdrup balance). In most of the coupled parameter space, however, these modes are not well separated and are best understood as *mixed SST/ocean-dynamics modes.* We note that in many regimes, the participation of subsurface dynamics, while important, bears little physical relation to the uncoupled ocean-dynamics modes. When the modes are traced in parameter space, it is possible to move continuously from a surface of eigenvalues originally characterized as an SST mode to one originally characterized as an ocean-dynamics mode. Singularities involving algebraic degeneracies of multiplicity two (we use the abbreviation "2-degeneracies" hereafter) subdivide the parameter space into regions of qualitatively different behavior and a 3-degeneracy plays a pivotal role in the merger of the eigensurfaces.

To better understand the balances involved in the merger of these modes, here and in Part III (Jin and Neelin 1993b) we approach the problem analytically so far as possible, in various limits, before resorting to numerical solution. In N91, this analysis was carried out for the much simpler zonally periodic case; here we examine the realistic case of an ocean basin with finite zonal extent. The response of a shallow-water ocean basin to specified wind stress of constant zonal structure and a given frequency has been examined by Cane and Sarachik (1981, CS81 hereafter). For the coupled problem at hand, we need to know the response of the ocean to a wind stress whose complex frequency/growth rate and zonal structure are *internally* determined by the coupled system. Making use of results from CS81 and Cane and Moore (1981), we derive a Green's function for the ocean response to coupled wind stress for a given temporal eigenvalue. Combined with the SST equation and atmospheric model of Part I, the eigenvalue problem is thus formulated in terms of integral operators in x that provide a good basis for making approximations.

The model in its basic form is given in section 2, along with the nondimensionalization that leads to the definition of important parameters for the coupled system. Section 3 gives the Green's function derivation, a compact statement of the integral formulation of the coupled eigenvalue problem, a brief summary of the uncoupled modes, and a discussion of the implications of filtering out the scattering spectrum. Inspection of the eigenvalue problem suggests various limits near which approximations may be applied to yield analytic or near-analytic results. These provide insight into the coupled dynamics that obtain in various regions of the parameter space. At the end of section 3, we define the limits to be considered and outline their respective regions of validity in parameter space. Our strategy is to seek analytic solutions in regions that surround the complicated region where the degeneracies occur. Part III pursues this strategy for cases in which coupling can be order unity or larger, while the remainder of this paper examines the weak-coupling limit. Section 4 gives series solutions in the weak-coupling limit and employs them, for instance, to argue roughly where in parameter space the transition occurs between weakly modified ocean-dynamics modes and mixed SST/ocean-dynamics modes. Summary and discussion are provided in section 5.

2. The model

a. Model equations

The model used here is closely related to the model employed in Part I and that of N91, which can be thought of as a "stripped-down" version of the Zebiak and Cane (1987) model. Here we concentrate on the analysis of the eigenmodes of the model linearized about climatology.

The SST equation for the equatorial band, linearized about a basic state with mean upwelling, can be written as

$$\partial_t T' + u'_m \partial_x \bar{T} + w'_m \partial_z \bar{T} + \frac{\bar{w}}{H_{1\,1/2}} (T' - \gamma_o h') + u'_s \partial_x \bar{T} + w'_s \partial_z \bar{T} + \epsilon_T T' + \kappa \partial_x^2 T' + \bar{u}_1 \partial_x T' = 0. \quad (2.1)$$

Here $\partial_z \bar{T} = (\bar{T} - \bar{T}_{\text{sub}})/H_{1\,1/2}$ and $\gamma_0 = (\partial_h T_{\text{sub}})|_{h=\bar{h}}$, where T_{sub} is subsurface temperature parameterized as a function of h [see Eq. (2) of Part I] and $H_{1\,1/2}$ is the depth scale characterizing upwelling of the subsurface temperature; $\bar{u}_1$ is the zonal current of the basic

state in the surface layer. The effects of meridional advection are implicit in the vertical advection terms when $\bar{w} > 0$ (see N91, Appendix) and their effects in possible regions of $\bar{w} < 0$ are neglected, as indicated by the numerical results of Part I. In numerical and nonlinear work, we use an analytic version of the Heaviside function, $\mathscr{H}(w)$, to ensure that all bifurcations can be brought into normal form. Here, we simply set $\mathscr{H}(\bar{w}) = 1$ and neglect $d\mathscr{H}/dw|_{\bar{w}}$.

The currents in the surface layer have two components:

$$u'_1 = u'_s + u'_m, \quad w'_1 = w'_s + w'_m$$

with subscript m denoting the part due to the vertical mean currents above the thermocline and subscript s denoting the part due to the vertical shear currents associated with the fixed-depth surface layer. The vertical mean currents and thermocline depth perturbations are governed by the usual linear, reduced-gravity, shallow-water ocean dynamics, with

$$w'_m = H_1(\partial_x u'_m + \partial_y v'_m). \tag{2.2}$$

The vertical shear currents associated with the active surface layer are given along the equatorial strip by

$$u'_s = b_u \frac{\tau'_e}{\rho H}$$

$$w'_s = (-b_w + H_1 b_u \partial_x) \frac{\tau'_e}{\rho H} \tag{2.3}$$

where $b_w = (H - H_1)\beta/\epsilon_s^2$ and $b_u = (L_s/H_1)b_w$ and τ'_e denotes the equatorial value of τ'. Here ϵ_s is a strong damping coefficient for the vertical shear currents. The b_w term dominates; that is, w'_s is largely produced by Ekman pumping due to β at the equator. We use "active surface layer" to refer to feedbacks associated with this component of the surface currents that are explicitly due to the momentum transfer between the surface layer and the remainder of the shallow-water layer. We avoid the term "mixed layer" since this commonly refers to density: the entire shallow-water layer is mixed in density but not in momentum.

The atmospheric model may be written

$$\frac{1}{\rho H}\tau' = \mu \mathscr{A}(T'; x, y), \tag{2.4}$$

where $\mathscr{A}(T')$ is a linear but nonlocal function of T' over the entire basin. For a Gill (1980) model, and with a specified meridional profile of the forcing, $\mathscr{A}$ is a simple integral operator. The relative coupling coefficient, μ, is discussed below.

1) NONDIMENSIONALIZATION

The nondimensionalization is a more straightforward version of that used in N91. Table 1 summarizes the scales employed and how each variable is scaled; the most important parameters for exploring the properties of the coupled system are distilled from these in section 2a(3). For the shallow-water subsystem, an anisotropic scaling is used, with the basin length L used for x scaling and the radius of deformation, L_D, used for y scaling. Dropping terms $O((L_D/L)^2)$ and $O(L_D/L)$ yields the equatorial long-wave approximation with meridional wind stress neglected. The main oceanic time scale is the time scale of Kelvin wave propagation across the basin,

$$t_c \equiv L/c_o,$$

which measures the rate of oceanic adjustment. The acceleration scale due to wind stress acting on the shal-

TABLE 1. Scales used in nondimensionalization. Numerical values used in estimating time scales are provided in brackets.

Primary scales	
$L_D \equiv (c_o/\beta)^{1/2}$	oceanic radius of deformation
L	zonal basin length (1.5×10^7 m)
$c_o = (gH)^{1/2}$	oceanic Kelvin wave speed (2.7 m s^{-1})
H	mean thermocline depth (150 m)
A	scale of atmospheric model A: wind stress acceleration on ocean per unit SST anomaly
ΔT	scale of SST: related to temperature differences accessible in basic state (4–5 K)
$t_c \equiv L/c_o$	time scale of ocean adjustment *in zonal direction* by equatorial waves
$t_s \equiv (b_w A \Delta T/H_{1\,1/2})^{-1}$	coupled time scale of SST change by surface-layer current perturbations
t_T	net time scale of adjustment by SST
Additional scales	
$A\Delta T$	acceleration scale due to wind stress perturbations on ocean (2×10^{-7} m s^{-2} corresponds to 0.03 Pa stress anomalies for realizable SST nomalies)
$U = A\Delta T t_c$	scale of vertical-mean zonal currents, u'_m
$c_o U g^{-1} = A\Delta T L g^{-1}$	scale of thermocline perturbations, h'
UH_1L^{-1}	scale of upwelling due to vertical mean motions, w'_m
$b_w A\Delta T$	scale of upwelling due to surface layer, w'_s
$b_w A\Delta T L_s/L$	scale of zonal currents due to surface layer, u'_s
b_w	coefficient of surface-layer upwelling (60 s corresponds to 0.05 Pa stress giving 1.5 m day^{-1} upwelling)
H_1	depth of surface layer (40 m)
$H_{1\,1/2}$	depth for finite differencing between surface and subsurface (75 m)
$L_s = \epsilon_s/\beta$	damping length scale for surface layer
L_a	scale of atmospheric y variation
$t_m \equiv c_o(A\Delta T)^{-1}$	coupled time scale of SST change by vertical mean current perturbations
$t_w \equiv [\text{mag}(\bar{w}/H_{1\,1/2})]^{-1}$	time scale due to mean upwelling (75 m/1.5 m day^{-1} $\sim$ 50 days)
$t_h \equiv t_m t_w t_c^{-1} \times [\text{mag}(\gamma_0(x)H/\Delta T)]^{-1}$	coupled time scale of SST change due to thermocline perturbations (mag(γ_0) $\sim$ .05 K m^{-1})

low-water ocean is $A\Delta T$ where A is the wind stress acceleration per unit SST anomaly produced by the atmospheric feedback and ΔT is the SST scale. The zonal current scale, U, is the scale of currents that can be accelerated in time t_c and is relevant to the transition between the weak-coupling and strong-coupling limits. It is consistent with the scale of thermocline perturbations, $A\Delta TL/g$, which is appropriate to the Sverdrup balance.

Let mag( ) denote a typical magnitude of a quantity across the basin. We use $\Delta T/L$ for mag$(\partial_x \bar{T})$ and $\Delta T/H_{1\,1/2}$ for mag$[(\bar{T}-\bar{T}_{\rm sub})/H_{1\,1/2}]$. Using the same ΔT for these two related quantities is reasonable for realistic basic states, even though the former is characterized by the difference between the warmest water and $\bar{T}$ in the cold tongue, while the latter is characterized by the difference between $\bar{T}$ and subsurface temperature. In the nonlinear case, these also bracket the range of possible SST anomalies (warm and cold, respectively). In the linear case, ΔT is chosen to characterize the basic state but is also used for the perturbations since the latter can be rescaled by any arbitrary factor.

In nondimensionalizing the SST equation, we find four important time scales affecting SST through the various terms in the SST equation. One is the time scale associated with the mean upwelling,

$$t_w \equiv [\text{mag}(\bar{w}/H_{1\,1/2})]^{-1}.$$

This is the time scale over which water in the equatorial band is replaced by the combined effects of upwelling and meridional advection. Taking a value of $\bar{w}$ characteristic of the width of the band gives a time scale on the order of two months. The meridional scaling $\bar{v}/L_s$ gives the same time scale since $\bar{v}$ and $\bar{w}$ are linked by the continuity equation. The other three are coupled time scales:

$$t_m \equiv c_o(A\Delta T)^{-1}$$

is the time scale of SST change by coupled feedback through vertical mean currents in the terms $u'_m\partial_x\bar{T}$ and $w'_m\partial_z\bar{T}$. This scale is suitable for both processes, although the latter is smaller by a factor of $H_1/H_{1\,1/2}$. Typical parameters yield $t_m \sim 150$ days. This time scale also appears in the "thermocline feedback" time scale, but modified by other factors. Here

$$t_h \equiv t_m \frac{t_w}{t_c}[\text{mag}(\gamma_o(x)H/\Delta T)]^{-1}$$

is the time scale of SST change by the thermocline feedback, through the term $(\bar{w}/H_{1\,1/2})\gamma_o h'$. Typical parameters yield $t_h \sim 75$ to 100 days. Last,

$$t_s \equiv H_{1\,1/2}(b_w A\Delta T)^{-1}$$

is the time scale of SST change by feedback through surface-layer Ekman currents in the terms $w'_s\partial_z\bar{T}$ and $u'_s\partial_x\bar{T}$. The time scale characterizes the first process; the latter is a factor of L_s/L smaller but both act in the same manner in the coupling. Typical parameters yield $t_s \sim 70$ days.

We define the time scale of SST evolution, t_T, to be the *net* time scale resulting from the combination of these processes. In limits where there is a clear separation between the importance of the processes, t_T will be the dominant time scale, $t_T \to \min(t_m, t_h, t_s, t_w)$. In the general case where several processes enter, the order of magnitude of t_T can be estimated from these, although it must be borne in mind that some terms tend to cancel. For instance, the damping term ϵ_w, acting with time scale t_w, is canceled by the growth tendency due to all the other terms at the bifurcation. It is also worth recalling that the time scales defined here are appropriate to the temporal eigenvalues, that is, frequency and growth rate, and that frequencies of order $(100\text{ days})^{-1}$ correspond to periods on the order of two years. Conversely, the Kelvin wave basin crossing time, t_c, is indeed an appropriate time scale to nondimensionalize uncoupled ocean eigenvalues, since a period of four times this arises in the basin, and this corresponds to a frequency of $\pi/2$, in units of t_c^{-1}, which is suitably close to unity.

2) NONDIMENSIONAL EQUATIONS

Applying the above nondimensionalization and definitions, and dropping primes from perturbation variables, we obtain a coupled system:

$$\partial_t T = a(x)u_e - a_w(x)w_e + \gamma(x)h_e - \epsilon_w(x)T + \mu\delta_s b(x)\mathcal{A}_e(T;x) + \kappa\partial_x^2 T \quad (2.5)$$

$$(\delta\partial_t + r)u_m - yv_m + \partial_x h = \mu\mathcal{A}(T;x,y)$$

$$yu_m + \partial_y h = 0$$

$$(\delta\partial_t + r)h + \partial_x u_m + \partial_y v_m = 0, \quad (2.6)$$

where u_e, w_e, h_e, and $\mathcal{A}_e$ denote the equatorial values of u_m, w_m, h, and $\mathcal{A}$; where

$$\delta \equiv \frac{t_c}{t_T}$$

$$\delta_s \equiv \frac{t_m}{t_s} = b_w c_o/H_{1\,1/2} \quad (2.7)$$

and

$$a(x) = \frac{t_T}{t_m}\left(-\frac{L}{\Delta T}\partial_x\bar{T}\right)$$

$$a_w(x) = \frac{t_T}{t_m}\left(\frac{H_1}{\Delta T}\frac{\bar{T}-\bar{T}_{\rm sub}}{H_{1\,1/2}}\right)$$

$$\gamma(x) = \frac{t_T}{t_m}\left(t_c\frac{\bar{w}(x)}{H_{1\,1/2}}\frac{\gamma_o}{\Delta T/H}\right)$$

$$b(x) = \frac{t_T}{t_m}\left[\frac{\bar{T}-\bar{T}_{\rm sub}}{\Delta T} + \frac{H_{1\,1/2}}{H_1}\frac{L_s}{L}(-(L/\Delta T)\partial_x\bar{T})\right]$$

$$\epsilon_w(x) = t_T(\bar{w}/H_{1\,1/2} + \epsilon_T). \quad (2.8)$$

The coefficients on the lhs are nondimenisonal, while all terms on the rhs of (2.8) are dimensional. The coefficient $b(x)$ combines the effects of both $u_s'\partial_x\bar{T}$ and $w_s'\partial_z\bar{T}$, where the relatively small $\partial_x\mathcal{A}$ term has been dropped from the latter. The zonal advection term $\bar{u}_1\partial_x T$ has been dropped since it is not a fundamental source of instability and only gives rise to minor quantitative changes in numerical results. The coefficients $a(x)$ and $\gamma(x)$ represent zonal advection by anomalous vertical mean currents and the thermocline feedback through mean vertical advection of anomalous subsurface temperatures, respectively. The combined damping effects on equatorial SST of the basic-state vertical advection and Newtonian damping (due to surface heat fluxes) are represented by $\epsilon_w(x)$. The damping time scale, r, of the shallow-water ocean dynamics is nondimensionalized by t_c. Typical values of the coefficients in (2.8) are all near unity except $a_w(x) < 1$. A more detailed treatment of meridional advection terms would modify some of these coefficients and can introduce additional effects into the SST modes in specific physical situations (Barnett et al. 1991) but will not influence the qualitative behavior of the system as a whole, especially in terms of the relationship among different kinds of modes.

In most of our analysis, we will drop the horizontal diffusion term (and the insulating boundary conditions in x that accompany it) since typical values of κ, nondimensionalized by t_T/L^2, are $O(10^{-4})$. This term ensures that the system is well behaved and that the SST zonal eigenmodes are well defined in the low coupling limit. While diffusion will always affect the smallest-scale x eigenmodes, we will be concerned almost exclusively with the spatially gravest coupled modes for which the effect of this term is negligible, as can be verified a posteriori. We will also drop the a_w term (which is the vertical advection due to the divergence vertically averaged over the two layers) in most of our analysis for the sake of simplicity. This term can be combined with the h term, using $w_e = -(\delta\partial_t + r)h_e$, but is small whenever the temporal eigenvalue is small. In the periodic-basin case considered by N91, where frequencies of the uncoupled ocean modes are higher, it was found to be potentially important to some modes, but in the numerical work of Part I, it was found to be unimportant for realistic parameters in the basin case.

In explicitly specifying the atmospheric model, the simplest to work with is the case where only the zeroth Hermite function is retained in the y structure of the forcing in the atmospheric model. The equatorial value is

$$\mathcal{A}_e(T; x) = A_0\epsilon_a\left[\frac{3}{2}\exp(3\epsilon_a x)\int_x^1 \exp(-3\epsilon_a s)T\,ds - \frac{1}{2}\exp(-\epsilon_a x)\int_0^x \exp(\epsilon_a s)T\,ds\right], \quad (2.9)$$

where ϵ_a is proportional to the atmospheric boundary-layer damping rate, here written as the inverse spatial decay scale nondimensionalized by the ocean basin length. The atmosphere has an infinite extent in x (i.e., much larger than ϵ_a^{-1}). The boundary conditions used in deriving (2.9) are that anomalous forcing is zero outside of the ocean basin. The nondimensional parameter A_0 is a constant factor required to make the operator order unity for standard values of ϵ_a and reasonable SST configurations. A simple measure of $\mathcal{A}_e$ relevant to the coupled problem is the stress produced by a constant SST anomaly in a region of length Δx, integrated over the region:

$$\frac{1}{2}A_0\epsilon_a^{-1}\left[\frac{2}{3} - \exp(-\epsilon_a\Delta x) + \frac{1}{3}\exp(-3\epsilon_a\Delta x)\right] \approx A_0/13$$

for $\epsilon_a\Delta x = 1$, which corresponds to an SST anomaly 7500 km long for a standard value $\epsilon_a = 2$. We use $A_0 = 15$ in all figures; a different A_0 would simply rescale μ. As $\epsilon_a \to 0$, (2.9) implies that $\mathcal{A}_e \to O(\epsilon_a)$, as is appropriate for the wind stress. The wind itself remains finite as the drag vanishes. Although the strength of coupling becomes small for small ϵ_a, we will often find it convenient to consider this limit for the spatial structure, leaving aside the influence on the coupling strength.

We further introduce the simplification of separability in the wind stress,

$$\mathcal{A}(T; x, y) = \mathcal{A}_e(T; x)Y(y).$$

Because the atmospheric y scales are much larger than the oceanic radius of deformation, the case of y-indepedent stress, $Y(y) = 1$, is a useful first approximation that results in great simplifications.

3) PARAMETERS

Among the many parameters lurking in the coupled system, we choose a simple set of primary parameters by which to examine (i) the relation between the uncoupled system and the fully coupled system, (ii) the contrast between time scales arising from the adjustment processes in the shallow-water subsystem and those arising from the SST equation, (iii) the distinction between the effects associated with the active surface layer and those associated with the shallow-water subsystem, (iv) the sensitivity to spatial effects in the atmospheric model, and (v) the effects of damping in both the shallow-water subsystem and SST equation. The first three parameters arise from the nondimensionalization; the last three are nondimensionalized versions of parameters that were explicitly present in the original equations.

The two most important parameters for this study are the following.

μ: The relative coupling coefficient—strength of the wind stress feedback from the atmosphere to the ocean relative to its standard value. For $\mu = 0$ the model is uncoupled; for $\mu = 1$ it has standard coupling for which the atmospheric feedback has magnitude A.

δ: The relative adjustment time coefficient—measures the ratio of the time scale of oceanic adjustment (in the zonal direction) by wave dynamics to the time scale of adjustment of SST by coupled feedback and damping processes. In Part I, we defined this parameter to be unity at standard values of all coefficients.

The two other primary parameters are

δ_s: The surface-layer coefficient—the ratio of the time scale of SST change by vertical-mean current and thermocline feedbacks to the time scale of SST change by coupled current perturbations associated with the active surface layer. It measures the importance of feedbacks due to the active surface layer: for $t_s \to \infty$, that is, when the surface-layer currents are unimportant, $\delta_s \to 0$; for $t_s \to 0$, that is, when the surface-layer current terms dominate in the SST equation, δ_s becomes large. In (2.8), the coefficients $a(x)$, $\gamma(x)$, $b(x)$, etc., all have similar scaling in t_T/t_m since we will concentrate on cases where the surface layer is unimportant. When the surface layer dominates, $\delta_s b(x)$ gives order unity time rate of change, while the other feedback terms are small. In Part I, we defined this parameter to be unity at standard values of all coefficients.

ϵ_a: The atmospheric damping length relative to the zonal basin scale; when $\epsilon_a = 1$, the westward decay scale in the atmosphere covers one-third of the basin. In addition to controlling the length scale over which SST anomalies influence wind stress, it affects the zonal phase of the stress anomalies relative to the SST anomalies to some extent: for sinusoidal anomalies, westerly winds lag warm SST by 90° of phase for small ϵ_a, and approaching 60° of phase for the largest physically reasonable values of ϵ_a.

The time scales arising from the SST equation and from the shallow-water subsystem are all of similar magnitude, so μ, δ, and δ_s are all of order unity for the most realistic case. We explore a number of limits where these parameters range from approaching zero to very large values. These limits are of interest insofar as they permit simplifications that assist in understanding the order unity case.

Two additional parameters are considered that are physically important and represent no additional burden in the analysis: namely, the damping terms, r, from the shallow-water equations and ϵ_T, which contributes a constant part to ϵ_w in the SST equation. We will make the reasonable assumption $r \ll 1$ in some cases. Some limits of interest, for instance, those involving low frequency, are sensitive. In such cases, we take the limit first with $r \neq 0$ and then consider small r if appropriate. The damping parameters also provide a straightforward connection between the discussion of eigenvalue degeneracies and higher codimension bifurcations, as outlined in Part I.

3. Green's function formulation of the coupled eigenvalue problem

We seek the eigenmodes of the coupled system in a finite ocean basin; the time dependence of all variables is of the form $\exp(\sigma t)$, where σ is the temporal eigenvalue. It is in general complex, with $\mathrm{Re}(\sigma)$ and $\mathrm{Im}(\sigma)$ giving the growth rate and frequency, respectively. Eigenmodes for which σ has an imaginary part always occur in conjugate pairs.

The response of an equatorial ocean basin to purely periodic wind stress of a given spatial structure is well known. Philander and Pacanowski (1980), for instance, consider a periodically forced OGCM, while CS81 derive analytic results for the shallow-water system in the case of wind stress constant in x and Gaussian in y. Analytic results are easily generalized to the case of complex σ as required for the eigenvalue problem where σ is internally determined. Such an approach has been used by Cane et al. (1990, CMZ hereafter) for a model where coupling occurs only through the value of h at the eastern boundary and where the wind stress is assumed to have fixed spatial form, constant in longitude in a specified region.

For the general case considered here, the zonal structure is internally determined by the eigenvalue problem, and coupling occurs along the equator throughout the basin. We thus need the ocean response in both u_m and h at the equator as a function of longitude for an arbitrary x dependence of wind stress. This is relatively easy to handle, at least for simple y structures of the wind stress. We obtain the (nontrivial) y structure of the ocean response as a by-product in the derivation, although this is not explicitly needed in the eigensystem.

a. *Green's function derivation*

As a basis for analytic solutions to the coupled eigenvalue problem, we require the oceanic response to a wind stress forcing of the form

$$\frac{1}{\rho H}\tau'(x, y; t) = e^{\sigma t}\mathcal{A}_e(x)Y(y),$$

where σ is in general complex and the x dependence of stress is to be determined internally by the eigenvalue problem. This is best approached using the Green's function for a forcing localized in x, but with a specified y structure. The derivation amounts to retracing the steps of CS81 with delta function forcing in x. Such a Green's function is not currently available in the literature; a Green's function for forcing local in x and y has been derived by Kuklinski (1984) and a Green's function for the value of h at the eastern coast is pro-

vided by CMZ, while a related time-domain Green's function for h is given in Schopf and Suarez (1990). Here we give a derivation for the special case of y-independent forcing that is greatly abbreviated by using results from Cane and Moore (1981, CM81 hereafter). The results of CMZ suggest that y dependence in the stress can be quantitatively important in some cases but we find that the important qualitative behavior of the system is captured without it.

We define the Green's function $\mathbf{G}(x, x_o, y)$ as a vector with u and h components such that

$$\mathbf{u}(x, y, t) = e^{\sigma t} \int_0^1 \mathcal{A}_e(x_o)\mathbf{G}(x, x_o, y)dx_o, \quad (3.1)$$

where $\mathbf{u} = [u(x, y, t), h(x, y, t)]^T$, and x is nondimensionalized by the basin width, L, as outlined above. The directly forced part of the Green's function, not satisfying boundary conditions, is

$$\mathbf{G}^{\text{forced}}(x, x_o, y) = (1 - \mathscr{H}(x_0 - x))d_K\mathbf{M}_K \exp[-i\phi(x - x_0)] + \mathscr{H}(x_0 - x) \sum_{n=0}^{N} (2n + 1)r_n\mathbf{R}_n \times \exp[i\phi(x - x_0)(2n + 1)] \quad (3.2)$$

where $\mathscr{H}(x_0 - x) = 1$ for $x_0 > x$, zero otherwise, is the Heaviside function, and d_K and r_n are the forced Kelvin and Rossby wave coefficients corresponding to $Y(y)$; $\mathbf{M}_K$ and $\mathbf{R}_n$ are the normalized Kelvin and Rossby vector functions defined by CS81 and given for reference in appendix B. We have defined

$$\phi = -i(\delta\sigma + r) \quad (3.3)$$

to include both the eigenvalue times the relative time scale parameter from (2.7) and oceanic damping, r, choosing the complex phase of ϕ for consistency with CM81. As discussed in CS81, when using the long-wave approximation in the inviscid case, the sums should strictly speaking be truncated at a finite N, which depends on the forcing frequency, although little error results from letting $N \to \infty$ when the frequency is fixed. In our case, where both damping and complex frequency are included, it is justifiable to let $N \to \infty$ whenever $\text{Re}(\sigma) \geq -r/\delta$; that is, that the mode does not decay faster than the damping time scale.

To the east of the forcing there is only the Kelvin wave in the directly forced solution. The sum of a Kelvin wave plus its eastern boundary reflection as Rossby waves, satisfying the condition $u = 0$ at $x = 1$, may be written,

$$\mathbf{K}_N(\phi(x - 1), y) \equiv \mathbf{M}_K e^{-i\phi(x-1)} + \sum_{n=0}^{(N-1)/2} 2\alpha_{2n+1}\mathbf{R}_{2n+1}e^{i\phi(x-1)(4n+3)} \quad (3.4)$$

where $\alpha_{2n+1} = (2^n n!)^{-1}[(2n + 1)!]^{1/2}$. Writing the Green's function in terms of $\mathbf{K}_N$ proves useful because there exists a simple closed form solution, derived by CM81 for the sum $\mathbf{K} \equiv \lim_{N\to\infty}\mathbf{K}_N$. The directly forced Kelvin wave plus its reflection in the region $x > x_0$ will just be $d_K e^{i\phi(x_0-1)}K_N(\phi(x - 1))$. To this must be added an additional Kelvin wave, plus its eastern boundary reflection, which is needed to satisfy the western boundary condition. Writing the coefficient of the sum of both Kelvin wave contributions as b_N, we have

$$G(x, x_0, y) = b_N K_N(\phi(x - 1), y) - d_K\mathscr{H}(x_0 - x)\mathbf{M}_K e^{-i\phi(x-x_0)} + \mathscr{H}(x_0 - x) \times \sum_{n=0}^{N} (2n - 1)\mathbf{R}_n r_n e^{i\phi(x-x_0)(2n+1)}. \quad (3.5)$$

The first two terms together represent the directly forced plus western boundary–reflected Kelvin waves (plus their eastern boundary reflections), the second term being simply due to the absence of a directly forced Kelvin wave west of x_0. The coefficient b_N is determined by the usual western boundary condition for the shallow-water equations in the long-wave approximation at $x = 0$:

$$\int_{-\infty}^{\infty} u(0, y)dy = 0. \quad (3.6)$$

The formal solution (3.5) is most useful when a simple closed form solution may be found for the sum. For the case $Y(y) = 1$, that is, forcing constant in y,

$$r_{2n+1} = -2\pi^{1/4}\alpha_{2n+1}(4n + 3)^{-1}, \quad r_{2n} = 0 \quad \text{and} \quad d_K = \pi^{1/4}.$$

The Rossby wave sum becomes simply

$$-\pi^{1/4}\{K_N(\phi(x - x_0, y)) - \mathbf{M}_K \exp[-i\phi(x - x_0)]\}$$

and the $\mathbf{M}_K$ term cancels the second term in (3.5), leaving

$$G(x, x_0, y) = b_N K_N(\phi(x - 1), y) - \pi^{1/4}\mathscr{H}(x_0 - x)\mathbf{K}_N(\phi(x - x_0), y). \quad (3.7)$$

This may be interpreted physically by noting that the jump in the u and h fields at x_0 for general $Y(y)$ is given by

$$\Delta u = \frac{d^2}{dy^2} Y(y), \qquad \Delta h = \left(1 - y\frac{d}{dy}\right)Y(y). \quad (3.8)$$

For the $Y(y) = 1$ case, this implies that the u velocities associated with the Rossby wave solution west of the forcing must sum to zero except for what can match the Kelvin wave solution to the east, while the height field matches the y-independent jump. The situation

is similar to having a wall that, instead of reflecting, emits the Kelvin wave eastward and the negative of its reflection westward.

Applying the boundary condition at $x = 0$,

$$b_N = \frac{\pi^{1/4}\int_{-\infty}^{\infty}(\mathbf{K}_N(-\phi x_0, y))_u dy}{\int_{-\infty}^{\infty}(\mathbf{K}_N(-\phi, y))_u dy} \quad (3.9)$$

where $(\mathbf{K}_N)_u$ indicates the u component of $\mathbf{K}_N$. When $\mathrm{Im}(\phi) < 0$, that is, the eigenvalue does not decay faster than r/δ, we can let $N \to \infty$ before taking the integral individually in numerator and denominator and make use of the closed form solution for $\mathbf{K}$, giving

$$\int_{-\infty}^{\infty}(\mathbf{K}(-\phi, y))_u dy = 2^{1/2}\pi^{1/4}(i\sin 2\phi)^{1/2},$$

$$b \equiv \lim_{N\to\infty} b_N = \pi^{1/4}\left(\frac{\sin 2\phi x_0}{\sin 2\phi}\right)^{1/2}. \quad (3.10)$$

For the case of strong decay, more careful treatment would be required.

The resulting Green's function is simply

$$\mathbf{G}(x, x_0, y) = \pi^{1/4}\left(\frac{\sin 2\phi x_0}{\sin 2\phi}\right)^{1/2}\mathbf{K}(\phi(x-1), y) - \pi^{1/4}\mathscr{H}(x_0 - x)\mathbf{K}(\phi(x - x_0), y) \quad (3.11)$$

where

$$\mathbf{K}(\phi\xi, y) = \pi^{-1/4}(\cos 2\phi\xi)^{-1/2} \times \exp\left[i\frac{y^2}{2}\tan 2\phi\xi\right]\begin{bmatrix} -i\sin 2\phi\xi \\ \cos 2\phi\xi \end{bmatrix}. \quad (3.12)$$

The properties of this closed form Green's function result in part from the fact that it filters out a class of rapidly decaying solutions related to the uncoupled scattering spectrum, while capturing modes that decay at the physical damping time scale or are destabilized by coupling. For modes that decay faster than $-r/\delta$, the convergence properties of the eigenvalue problem become quite subtle (see appendix A).

b. *Integral formulation of the eigenvalue problem*

The SST equation (2.5), combined with the equatorial values of u_e and h_e derived from (3.1) and (3.11)–(3.12) and the atmospheric integral operator, (2.9), constitutes an integro–differential formulation for the eigenvalue problem. The integral formulation for both the shallow-water subsystem and the atmospheric component is advantageous in this system because of the complexity of the boundary conditions for these. In working with the original differential form of the equations, it can be difficult to assess the correctness of approximations made locally when the effect of the boundaries is crucial. It is much more reliable to make approximations to the integral form, where the boundary conditions are already included. When we drop the diffusion term from the SST equation, we obtain a purely integral formulation.

Our eigenvalue problem is thus

$$\sigma T = a(x)u_e + \gamma(x)h_e - \epsilon_w(x)T + \mu\delta_s b(x)\mathcal{A}_e(T; x) \quad (3.13)$$

$$u_e = -i\mu\Big[\int_0^1\left(\frac{\sin 2\phi x_0}{\sin 2\phi}\right)^{1/2}\mathcal{A}_e(T; x_0)dx_0 \times(\cos 2\phi(x-1))^{-1/2}\sin 2\phi(x-1) - \int_x^1 \mathcal{A}_e(T; x_0)(\cos 2\phi(x - x_0))^{-1/2} \times \sin 2\phi(x - x_0)dx_0\Big]$$

$$h_e = \mu\Big[\int_0^1\left(\frac{\sin 2\phi x_0}{\sin 2\phi}\right)^{1/2}\mathcal{A}_e(T; x_0)dx_0 \times(\cos 2\phi(x-1))^{1/2} - \int_x^1 \mathcal{A}_e(T; x_0) \times(\cos 2\phi(x - x_0))^{1/2}dx_0\Big] \quad (3.14)$$

where $\phi = -i(\delta\sigma + r)$ from (3.3) and where the integral operator $\mathcal{A}_e(T; x)$ is given by (2.9).

The longitudinal dependence of the coefficients a, b, γ, and ϵ_w, is quantitatively and sometimes qualitatively important to the coupled modes in the basin. We will, however, often consider the special case where these are treated as constant. This facilitates analytical solution and also highlights the features of the spatial structure that are implied purely by the finite ocean basin. We find that the most important qualitative behavior of the system, the smooth joining of eigensurfaces associated with oceanic and SST time derivatives, is reproduced even in this very simplified case.

c. *Uncoupled modes*

For the uncoupled case, $\mu = 0$, the shallow-water subsystem and the SST equation separate, each determining a subset of the eigenvalues (ocean dynamics modes and SST modes, respectively).

In appendix A, we show that the ocean-dynamics spectrum in the long-wave approximation consists of the ocean basin modes of CM81 plus a discretized scattering spectrum. The ocean basin modes are exact modes in the long-wave approximation; otherwise they are slightly leaky due to the poleward loss by coastal Kelvin waves on the eastern boundary. While the scattering spectrum plus ocean basin modes arise in the truncated equations [e.g., (3.7) or (3.9)], the closed form of the summation (3.4) has poles corresponding only to the ocean basin modes, a filtering that is useful for our current approach.

The uncoupled SST modes are rather uninteresting, being just the familiar heat conduction equation solutions. Considering the simple case where ϵ_w is constant in x, the eigenfunctions are just

$$\cos(k\pi x/2), \quad k = 0, 1, 2, 3, \cdots$$

with all large-scale eigenvalues ($k \ll (\kappa/\epsilon_w)^{-1/2}$) giving decay at rate ϵ_w when κ is small. The diffusion term and insulation boundary conditions here serve in determining the eigenstructure by breaking a degeneracy, but do not significantly affect the eigenvalues for the large-scale modes.

d. *Useful limits*

The μ–δ parameter plane will be of particular interest in examining the coupled problem; the range $[0, \infty)$ is considered for both the relative coupling coefficient, μ, and the relative adjustment time coefficient, δ. Various useful limiting cases occur in regions that roughly correspond to the four boundaries of this quadrant. We use the following terminology for the cases to be pursued both here and in Part III.

- The fast-wave limit: for small δ, where the time scale of ocean adjustment by wave dynamics is fast compared to the time scale of change of SST by coupled and damping processes.
- The fast-SST limit: for large δ, where the time scale of SST change is fast compared to the time scale of ocean adjustment, the converse of the fast-wave limit.
- The weak-coupling limit: for small μ, where the coupling is sufficiently weak that the coupled modes are closely related to the modes of the uncoupled system.
- The strong-coupling limit: for large μ, where coupling dominates in oceanic balances.

The regions of validity of the approximations made in these limits depend on the properties of the system and also on the specific eigensurface being approximated. Thus, the definitions of large and small in the above are left vague. Inspection of the coupled system (3.13)–(3.14) suggests that two cases will be useful in making approximations, $\delta\sigma \ll 1$ and $\delta\ \mathrm{Re}(\sigma) \gg 1$.

When $\delta\sigma \ll 1$, the ocean response (3.14) can be expanded in a Taylor series about $\delta\sigma = 0$, valid for the coupled SST modes. Since there is no difficulty in simply setting $\delta = 0$ for these modes, we will often refer to this as the fast-wave limit and use the terminology "near the fast-wave limit" for the neighboring, small-δ region of validity. For large coupling, SST mode eigenvalues are proportional to μ, so this region of validity is confined to $\mu\delta \ll 1$ at the large coupling end, while its extent is independent of μ at the small coupling end. For wave-related modes, the fast-wave limit is most conveniently considered by rescaling time by δ^{-1} and T by μ. The product $\mu\delta$ then appears multiplying all terms on the rhs of (3.13), and thus the regions of validity of the fast-wave limit and weak-coupling limit merge continuously for these modes. The hatched areas in Fig. 1 show these regions of validity schematically. Likewise, the regions of validity of the weak-coupling and fast-wave limits overlap for the SST modes.

When $\delta\ \mathrm{Re}(\sigma) \gg 1$, functional approximations to the ocean response (3.14) are possible and are valid for the unstable modes. Near the fast-wave limit, the eigenvalues are proportional to coupling, so the region of validity is confined to $\mu\delta \gg 1$, also shown in Fig. 1. There is thus no overlap of regions of validity of approximations made in the strong-coupling limit and the fast-wave limit. However, the two regions do approach each other for large coupling and small δ.

The strong-coupling limit does overlap the fast-SST limit. In the fast-SST limit, no useful approximations arise unless further assumptions are made. It does not yield any simplification in the complex oceanic response; it simplifies only the SST equation, which is already mathematically tractable. A very relevant particular case of the fast-SST limit is treated by CMZ and Schopf and Suarez (1990). Their models correspond to the case where $\gamma(x)$ and $\epsilon_w(x)$ are delta functions in x at the eastern boundary and all other terms are neglected in the SST equation, (3.13), with further simplification to the x structure of the winds. Since these are qualitatively reasonable approximations for some of the modes in question, we will mainly refer to CMZ for results in the fast-SST limit, although the connection of the fast-SST limit to the fast-wave limit at strong coupling is analyzed in Part III.

From Fig. 1, it may be seen that our various approximations almost completely surround the central region in the parameter plane (hatched) where the degeneracies found numerically in Part I occur. By de-

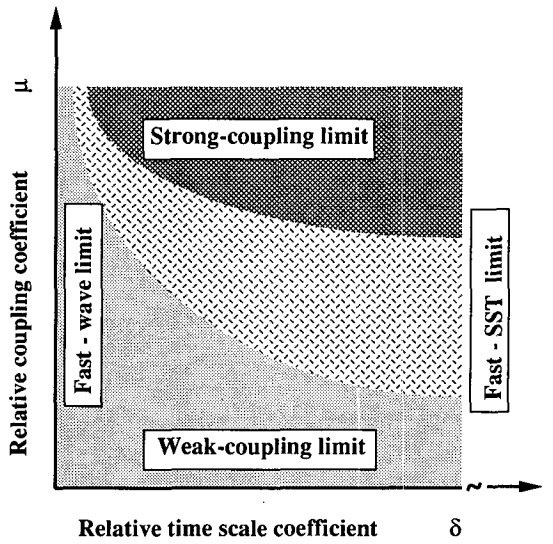

FIG. 1. Schematic regime diagram of the (μ, δ) parameter space showing regions of validity of various limits.

scribing the behavior in these various regions, we are thus able to sketch out a fairly complete picture of the parameter dependence of the modes in physical terms. The gap between the fast-wave limit and the strong-coupling limit is not fundamental in the sense that the eigensurfaces are smooth and continuous across the region and it is only the analytical approximations that are lacking. We will employ qualitative arguments to bridge this gap in Part III. The gap extending to the fast-SST limit is associated with the extension of the 2-degeneracies to this limit, as may be seen from the CMZ results.

We note that for numerical work, it can be useful to represent both the fast-wave limit and fast-SST limit at finite parameter values on the same diagram. A physically motivated transformation that accomplishes this is to nondimensionalize time by $(t_c + t_T)$ rather than t_T as used here. One then defines $\delta^* = \delta/(1 + \delta)$, which replaces δ in the shallow-water subsystem, while $(1 - \delta^*)$ appears in front of the SST time derivative. The fast-wave limit is still at $\delta^* = 0$, while the fast-SST limit occurs at $\delta^* = 1$, rather than at infinity, as in Fig. 1. Our use of δ is chosen for conceptual simplicity and is handy for analytic work since δ "tags" all shallow-water component time derivatives. The δ^* transformation will be used as necessary.

Our discussion of the μ–δ plane dependence is not complete in terms of the effects of the surface-layer processes. We consider primarily two cases:

- Case of an inactive surface layer: the limit $\delta_s \to 0$, where time scales of SST change by coupled advection processes due to perturbation currents from the active (in the sense of momentum transfer) surface layer are negligible. Advection processes due to the surface expression of perturbation vertical mean currents still occur, and the thermocline feedback is mediated by fixed climatological surface layer upwelling.
- Case of surface-layer processes only: we treat the case of an active surface layer in the limit of large δ_s, where other coupled processes are negligible. The fast-wave and fast-SST limits are then irrelevant since the dynamics of the shallow-water subsystem is unimportant.

The case of order unity δ_s is straightforward to treat in the fast-wave limit, but this transition is easily understood from the two limits and the periodic-basin results. We do treat the case of δ_s varying from zero to unity in the weak-coupling limit to provide an example of the transition.

4. The weak-coupling limit

Much of the current discussion about how the coupled system behaves has been based on terminology and intuition gained from the relatively well-understood uncoupled problem. A natural and useful limit to consider is therefore the weak coupling limit: $\mu \ll 1$. For sufficiently small coupling, the modification of the eigenvalues and eigenstructure relative to the uncoupled system may be assumed small and a perturbation method applied. From the numercial results in Part I, we may anticipate that this limit may not, in fact, be the most relevant to the coupled problem at realistic parameter values. Rather, it serves to provide a connection between the uncoupled case and the fully coupled problem.

a. *Modification of the ocean basin modes*

There is little point in attempting to expand about the uncoupled scattering spectrum, whose modes are not robustly defined even at $\mu = 0$. We focus on the ocean basin modes since these are structurally well defined at $\mu = 0$ and therefore offer the possibility that their properties may carry over to the weakly coupled problem. We can thus elaborate on the numerical indications from Part I that coupling tends to rapidly modify modal structure.

For simplicity, we consider the case of an inactive surface layer, $\delta_s = 0$, and concentrate on the modification of the ocean basin modes by feedbacks due to vertical mean currents and thermocline depth. In the coupled eigenvalue problem as $\mu \to 0$ a subset of the coupled modes matches smoothly to the uncoupled ocean basin modes discussed in section 3:

$$\phi \to \phi_k = \frac{k\pi}{2}, \quad k = 1, 2, 3, \cdots \tag{4.1}$$

with frequency σ_k, given by $\delta\sigma_k + r \equiv i\phi_k$, and

$$(u_e, h_e) \to (u_{ke}, h_{ke})e^{\sigma_k t} \tag{4.2}$$

aside from an arbitrary amplitude factor that has been set to unity. Here (u_{ke}, h_{ke}) are the (u, h) components of the free ocean basin mode structure evaluated at the equator:

$$u_{ke} = -i[\cos k\pi(x - 1)]^{-1/2} \sin k\pi(x - 1)$$
$$h_{ke} = [\cos k\pi(x - 1)]^{1/2}. \tag{4.3}$$

The SST component of these free ocean basin modes may be evaluated diagnostically as

$$T = T_k e^{\sigma_k t}$$
$$T_k = [au_{ke} + \gamma h_{ke}](\sigma_k + \epsilon_w)^{-1}. \tag{4.4}$$

Because the free ocean basin modes are easily recovered from the Green's function formulation of the eigenvalue problem (3.13)–(3.14), this provides a convenient basis for estimating modifications to the eigenvalue and eigenstructure at low coupling.

For $\mu \ll 1$, the SST component will create a correction to the structure of u_e and h_e along with a correction to the eigenvalue:

$$\sigma = \sigma_k + \sigma'(\mu), \quad |\sigma'| \ll |\sigma_k|$$

$$(u_e, h_e, T) = (u_{ke}, h_{ke}, T_k)e^{\sigma t} + O(\mu). \quad (4.5)$$

The first term, with the structure of the basin modes, arises from the contribution of the first terms in the Green's function expression of (u_e, h_e), respectively, in (3.14), with unit amplitude chosen; the second, $O(\mu)$ term, which is the structure change due to coupling, arises from the second terms in (3.14).

To include the effect of the structure change explicitly, we write the following expansion:

$$u_e = e^{\sigma t}\left\langle u_{ke} - \mu \int_x^1 \left[\sum_{n=0}^{\infty} \mathcal{A}_e(T_k^{(n)}; x_0)\mu^n\right]\{-i[\cos 2\phi(x - x_0)]^{-1/2} \sin 2\phi(x - x_0)\}\, dx_0\right\rangle$$

$$h_e = e^{\sigma t}\left[h_{ke} - \mu \int_x^1 \left[\sum_{n=0}^{\infty} \mathcal{A}_e(T_k^{(n)}; x_0)\mu^n\right][\cos 2\phi(x - x_0)]^{1/2} dx_0\right] \quad (4.6)$$

which gives, from (3.13),

$$T_k^{(n)}(x) = \frac{ia(x)}{\sigma + \epsilon_w} \int_x^1 \mathcal{A}_e(T_k^{(n-1)}; x_0)[\cos 2\phi(x - x_0)]^{-1/2} \sin 2\phi(x - x_0) dx_0$$

$$- \frac{\gamma(x)}{\sigma + \epsilon_w} \int_x^1 \mathcal{A}_e(T_k^{(n-1)}; x_0)[\cos 2\phi(x - x_0)]^{1/2} dx_0, \quad n \geq 1, \quad (4.7)$$

and $T_k^{(0)}$ is just given by the ocean basin mode SST structure, T_k, from (4.4); that is,

$$T_k^{(0)}(x) = \frac{-ia(x)}{\sigma + \epsilon_w}[\cos 2\phi(x - 1)]^{-1/2} \sin 2\phi(x - 1) + \frac{\gamma(x)}{\sigma + \epsilon_w}[\cos 2\phi(x - 1)]^{1/2}. \quad (4.8)$$

In this expansion, the modifications to the eigenstructure are expanded in orders of μ, while the eigenvalue μ dependence is not explicitly specified and will be determined internally in the solution. Substituting (4.6) into the Green's function formulation (3.14), we obtain an eigenvalue equation

$$1 = \mu \int_0^1 \left(\frac{\sin 2\phi x_0}{\sin 2\phi}\right)^{1/2} \mathcal{A}_e\left(\sum_{n=0}^{\infty} T_k^{(n)}(x_0)\mu^n; x_0\right) dx_0. \quad (4.9)$$

In combination with (4.7)–(4.8), this eigenvalue equation is a nonlinear function of σ and can be solved numerically when the series expansion for the structure is truncated at any given order. Note that (4.7) already takes into account the changes to (u_e, h_e) at each order, as given by (4.6).

The series solution given by (4.7)–(4.9) has a finite radius of convergence in μ, rather than being merely an asymptotic approximation, since the factor relating $T_k^{(n)}$ to $T_k^{(n-1)}$ in (4.7) is bounded for any reasonable spatial pattern. Although the radius of convergence is not easy to write explicitly in terms of the parameters, it is easy to see, in evaluating the solution numerically at higher orders, for which range of μ convergence is achieved rapidly and where it fails. The finite radius of convergence is, of course, itself symptomatic of the fundamental modifications that the fully coupled modes undergo, relative to the modes at weak coupling.

The system (4.6)–(4.9) provides a clear indication of how the eigenstructure of leading order, that is, the free ocean basin mode structure, and higher-order changes to the structure due to the coupling are both involved in determining σ', the eigenvalue correction in the weak-coupling limit. The series solution for the structure of the mode, (4.6)–(4.8), also makes it obvious that the changes to the structure produced by coupling are associated with the transition to a mode of mixed character. The time derivatives of the SST equation appear prominently in the denominators of (4.7) and (4.8), and hence in the correction terms of (4.6), and affect the solution of (4.7) to a greater degree as coupling increases. A case of particular interest is the solution when only the zeroth-order part of the structure expansion is retained; that is, only $T^{(0)}$ is retained in (4.8). We will refer to this as the order-zero solution, referring to the structure expansion, even though the eigenvalue correction depends on μ, because (4.6) does not give a simple ordering for σ' in μ. The eigenvalue problem for this case becomes

$$[\sin 2(\phi_k - i\delta\sigma')]^{1/2} = \mu \int_0^1 [\sin 2(\phi_k - i\delta\sigma')x_0]^{1/2} \times \mathcal{A}_e(T^{(0)}; x_0) dx_0 \quad (4.10)$$

with $T^{(0)}$ given by (4.8). The solution σ' represents the eigenvalue correction that would obtain if the coupling through SST is determined by the *structure* of the uncoupled mode. Even at this truncation, (4.10) is nonlinear in σ' and the corrections due to retaining terms of higher order are not simply additive. Nonetheless, for sufficiently small μ, (4.10) will constitute

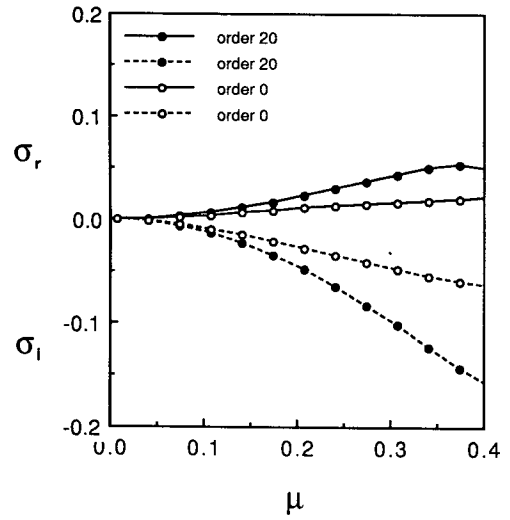

FIG. 2. Eigenvalue correction to the uncoupled ocean basin mode frequency for the gravest oscillatory coupled mode as a function of μ near the low coupling limit. Solid lines show growth rate, σ_r; dashed lines show frequency correction, σ_i. Open (solid) circles indicate solutions with the series expansion for the structure truncated at order zero (20) in μ. Coefficients used are $a = 1.0$, $\gamma = 1.0$, $\epsilon_w = 1.0$, $\epsilon_a = 2.0$, $\delta_s = 0$, $\delta = 3.0$.

a good approximation to the series solution. For μ small enough that $|\sigma'| \ll |\phi_k|$, (4.10) simplifies to

$$(-i2\delta\sigma')^{1/2} = \mu \int_0^1 (\sin k\pi x_0)^{1/2} \times \mathcal{A}_e(T^{(0)}|_{\phi=k\pi/2}; x_0)dx_0 \quad (4.11)$$

giving, for the case of constant a and γ,

$$2\delta\sigma' = i\mu^2(\sigma_k + \epsilon_w)^{-2}[-ia\Gamma_1 + \gamma\Gamma_2]^2 \quad (4.12)$$

where Γ_1 and Γ_2 are complex constants obtained by substituting (4.8) into (4.11) and evaluating the integrals. They are associated with the SST response at zeroth order to the u_e and h_e fields, respectively.

Numerically, we can trace the eigenvalue solution of (4.7)–(4.9) at any desired order. Figure 2 shows the correction to the uncoupled eigenvalue, σ', for the gravest spatial mode, which is the most affected by the coupling, for $\delta = 3$. It is clear that the growth rate increases with coupling, while the correction to the frequency becomes rapidly negative, reducing the frequency relative to the uncoupled ocean basin mode, as observed in Part I. The range of coupling shown in Fig. 2 lies entirely within the radius of convergence of (4.9). The two pairs of curves shown are for the eigenvalue correction calculated using order-zero truncation and order-20 truncation, respectively, the latter of which is essentially converged. The correction at first order given by (4.10) makes use of the spatial structure of the ocean basin mode in the zeroth-order temperature structure. This curve differs from the parabolic shape suggested by the simplest case, (4.12), at relatively low coupling. An even more telling sign of where the structure of the coupled mode begins to differ strongly from that of the ocean basin mode is where the order-zero and order-20 curves diverge. This shows where the higher-order correction terms of (4.6) enter sufficiently strongly to affect the eigenvalue. Although the boundary between the region where the mode can be thought of as an ocean basin mode, slightly modified by coupling, and the region where it must be considered a mixed SST/ocean-dynamics mode is not a sharp division, the value of the coupling where the two curves begin to diverge provides a good indication of this. In other words, the mode ceases to be closely related to an ocean basin mode and acquires a mixed character at rather low coupling, for relative coupling coefficient only slightly larger than $\mu = 0.1$.

To make this point more concretely, Fig. 3 and Fig. 4 show the eigenstructure of SST and h_e for $\mu = 0.1$ and 0.3, respectively. For μ very small, u_e and h_e are similar to the ocean basin mode structure obtained by Cane and Moore (1981), and this still holds roughly in Fig. 3. The SST structure is dominated by the effects of zonal advection in this case. For larger μ, the struc-

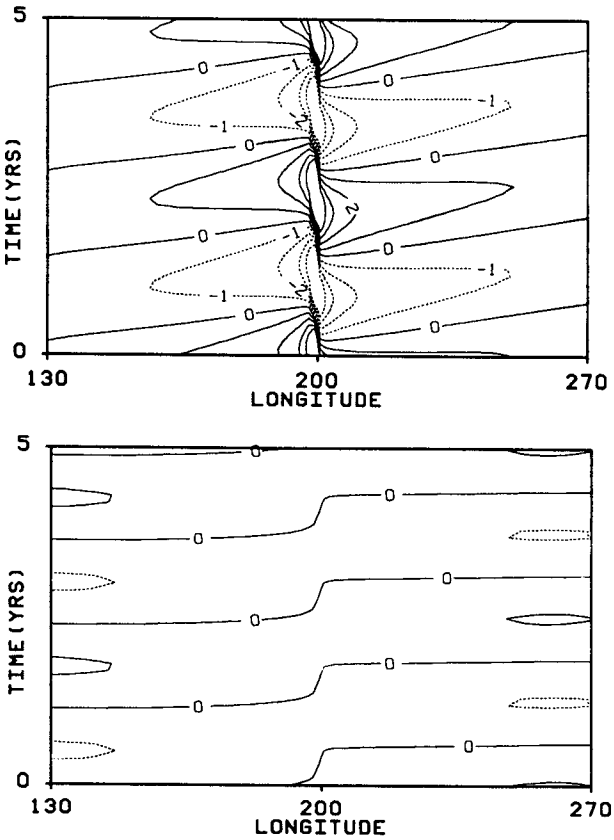

FIG. 3. Time–longitude dependence of the gravest oscillatory coupled mode (growth rate suppressed) along the equator for $\mu = 0.1$: (a) SST, (b) h_e.

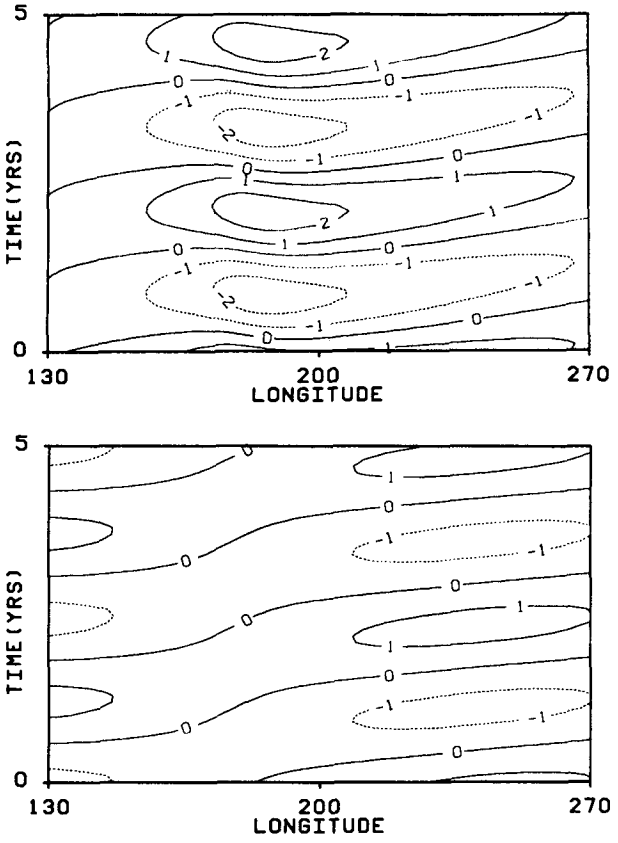

FIG. 4. As in Fig. 3 except for $\mu = 0.3$.

ture changes dramatically, as in Fig. 4. The modified coupled mode resembles the uncoupled mode very little, even though the frequency change is not yet large, about 30%. As the coupling reduces the frequency and introduces a growth rate, the form of the oceanic response evolves quickly away from the near-singular structure of the ocean basin mode and closer to the response to low-frequency forcing, with attendant changes in the patterns of advection and thermocline evolution affecting SST. The characteristic slow eastward "propagation" of the thermocline depth anomaly from west to east along the equator noted in Battisti (1988) and Chao and Philander (1993) begins to appear as the frequency decreases, as dictated by basin dynamics at low frequencies (CS81). The SST pattern has evolved to a smooth, basin-scale structure supported by both advection and thermocline feedbacks. It is easy to see, even at this modest coupling, that this mixed mode is taking on the characteristics of the SST mode with which it was seen to merge in Part I.

b. *Destabilization of SST modes*

The uncoupled SST modes discussed in section 3 decay at a rate dictated by basic-state local damping processes, ϵ_w, and satisfy insulation boundary conditions. In the weak coupling limit, where μ is small, these modes are effectively mixed to produce coupled SST modes for values of $\mu > O(\kappa)$. The coupling tends to destabilize these modes, reducing the decay rate; the range of validity of the approximate ends at smaller μ than where net instability occurs, but this limit permits an examination of the transition.

To obtain the eigenvalue solution of SST modes in the weak coupling limit, a different approach from the one employed for the oceanic basin modes is used. For small μ, the eigenvalue correction will be small so we will have

$$\sigma = -\epsilon_w + \sigma'(\mu). \tag{4.13}$$

The approximations we need to make are to the oceanic response, (3.14), so the relevant condition is $|\sigma'| \ll \epsilon_w$, which corresponds to the range of validity $\mu \ll O(\epsilon_w)$. The structure of SST modes at low coupling is a mixture of the uncoupled SST mode structures, so we write

$$T = [T_0(x) + O(\mu)]e^{\sigma t}$$

$$T_0(x) = \sum_{k=0}^{\infty} B_k \cos k\pi x. \tag{4.14}$$

The associated thermocline and vertical mean currents are only $O(\mu)$ at leading order, as seen by substituting (4.14) into (3.14). Using (4.13) and omitting the small term r due to oceanic damping, we obtain

$$u_e = \mu e^{\sigma t}\Bigg[\int_0^1 \left(\frac{\sinh 2\delta\epsilon_w x_0}{\sinh 2\delta\epsilon_w}\right)^{1/2} \mathcal{A}_e(T_0; x_0)dx_0 \times [\cosh 2\delta\epsilon_w(x-1)]^{-1/2} \sinh 2\delta\epsilon_w(x-1) - \int_x^1 [\cosh 2\delta\epsilon_w(x-x_0)]^{-1/2} \sinh 2\delta\epsilon_w(x-x_0) \times \mathcal{A}_e(T_0; x_0)dx_0\Bigg] + O(\mu^2)$$

$$h_e = \mu e^{\sigma t}\Bigg[\int_0^1 \left(\frac{\sinh 2\delta\epsilon_w x_0}{\sinh 2\delta\epsilon_w}\right)^{1/2} \mathcal{A}_e(T_0; x_0)dx_0 \times [\cosh 2\delta\epsilon_w(x-1)]^{1/2} - \int_x^1 [\cosh 2\delta\epsilon_w(x-x_0)]^{1/2} \times \mathcal{A}_e(T_0; x_0)dx_0\Bigg] + O(\mu^2). \tag{4.15}$$

Therefore to first order, using (3.13), the eigenvalue equation for SST modes in the low coupling limit can be written

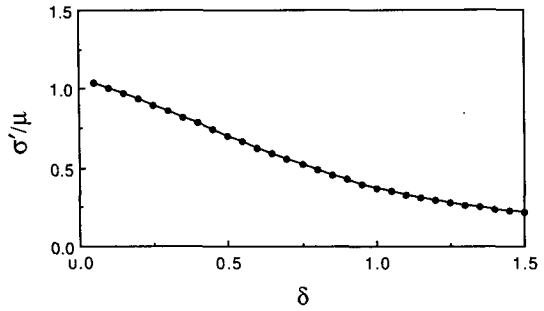

FIG. 5. Growth rate correction (scaled by μ) of the gravest stationary SST mode vs δ with $a = 0.5$, $\gamma = 1.0$, $\epsilon_w = 1.0$, $\epsilon_a = 2.0$, $\delta_s = 0.0$.

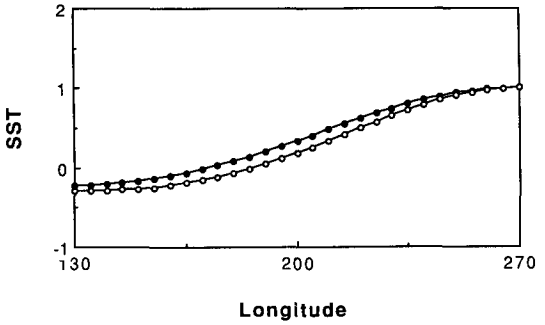

FIG. 6. SST structure of the gravest stationary SST mode for $\delta = 0.1$ (solid circles) and $\delta = 1.0$ (open circles).

$$\sigma' T_0(x) = \mu\delta_s b\mathcal{A}_e(T_0; x) + \mu a\Bigg[\int_0^1 \left(\frac{\sinh 2\delta\epsilon_w x_0}{\sinh 2\delta\epsilon_w}\right)^{1/2} \mathcal{A}_e(T_0; x_0)dx_0 \times [\cosh 2\delta\epsilon_w(x-1)]^{-1/2} \sinh 2\delta\epsilon_w(x-1) - \int_x^1 [\cosh 2\delta\epsilon_w(x-x_0)]^{-1/2} \sinh 2\delta\epsilon_w(x-x_0) \times \mathcal{A}_e(T_0; x_0)dx_0\Bigg] + \mu\gamma\Bigg[\int_0^1 \left(\frac{\sinh 2\delta\epsilon_w x_0}{\sinh 2\delta\epsilon_w}\right)^{1/2} \mathcal{A}_e(T_0; x_0)dx_0 \times [\cosh 2\delta\epsilon_w(x-1)]^{1/2} - \int_x^1 [\cosh 2\delta\epsilon_w(x-x_0)]^{1/2} \times \mathcal{A}_e(T_0; x_0)dx_0\Bigg] + \kappa\partial_x^2 T_0. \quad (4.16)$$

The $\kappa\partial_x^2 T_0$ term is included for completeness but makes no discernible difference for parameters of interest.

From (4.16), although it is clear that the eigenvalue correction σ' depends linearly on μ, it is still difficult to analytically obtain the eigenvalue and eigenstructure even in this simpler version of (3.13)–(3.14). A single term of the $\cos k\pi x$ series is not a solution for $\mu \neq 0$. To obtain the solution, we truncate the expansion for $T_0(x)$ in (4.14). Because $\{\cos k\pi x\}$ is a complete orthogonal base for the expansion, the rhs of (4.16) can also be expanded and so leads naturally to a spectral method of solution. With (4.14) truncated, (4.16) becomes a simple matrix eigenvalue problem. The real matrix includes the parameters a, b, and γ; in this approximation their x dependence can easily be included but we examine the case where they are treated as constant for simplicity.

The remaining parameters are δ and δ_s, while μ is only a scale factor for the eigenvalue correction. As $\delta \to 0$, the term associated with u_e disappears so that only the surface-layer processes and thermocline feedback contribute to the SST modes. In this case, analytical solutions are possible for the whole range of coupling, which will be analyzed in Part III. For $\delta \neq 0$, the solutions in this low coupling limit must be sought numerically. The results are shown in Figs. 5–8. Figure 5 shows the case with surface-layer processes shut off, $\delta_s = 0$. The gravest mode is nonoscillatory for the value of ϵ_a shown here and tends to be destabilized ($\sigma' > 0$). The eigenvalue correction for this stationary SST mode is not very sensitive to δ, as observed in Part I. The structure of this SST mode is shown in Fig. 6 for two values of δ. It is dominated by the first two terms of the $\{\cos k\pi x\}$ series with its amplitude largest in the eastern part of the basin. The structure is not sensitive to δ either, so we defer discussion of the east basin trapping to the fast-wave limit case in Part III, where dependence on ϵ_a and the possibility of eastward propagation will also be discussed.

As we increase δ_s from 0 to 1, we find that the first two stationary modes join and become an oscillatory mode that propagates westward. This is structurally similar to what was seen in Part I, where it was observed also at higher coupling. Figure 7 shows the eigenvalue correction of gravest mode as a function δ_s. The 2-degeneracy occurs at $\delta_s \approx 0.2$, and the frequency and

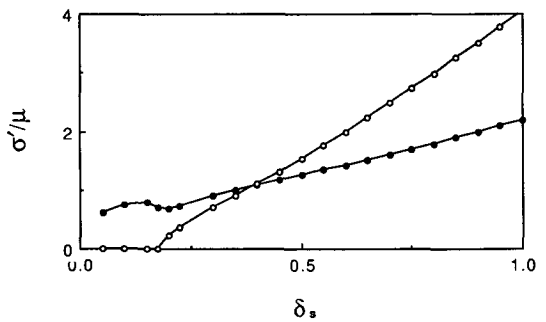

FIG. 7. Eigenvalue correction (scaled by μ) of the gravest stationary SST mode vs surface-layer coefficient, δ_s, with $a = 0.5$, $\gamma = 1.0$, $\epsilon_w = 1.0$, $\epsilon_a = 2.0$. Open (solid) circles show growth rate (frequency).

growth tendency, $\mathrm{Re}(\sigma')$, increase as δ_s increases. Thus the surface-layer processes tend to produce a westward-propagating SST mode as found in Part I. At low coupling the SST structure of this westward-propagating mode shows slight intensification toward the west in Fig. 8. This western basin amplification will be reduced at stronger coupling, as will be shown in Part III. The features of the mode in Fig. 8 are qualitatively consistent with those of Part I, although, of course, the numerical results in Part I included the inhomogeneity in the basic state that traps the SST perturbation toward the eastern basin.

The coupling thus dominates the structure of the SST modes even when it is weak in the sense that the modification to the uncoupled eigenvalue is small. The transition between the structure of the uncoupled SST modes and the coupled SST modes is confined to the region of truly tiny coupling, $\mu \ll \kappa$, for modes with x scales comparable to the basin.

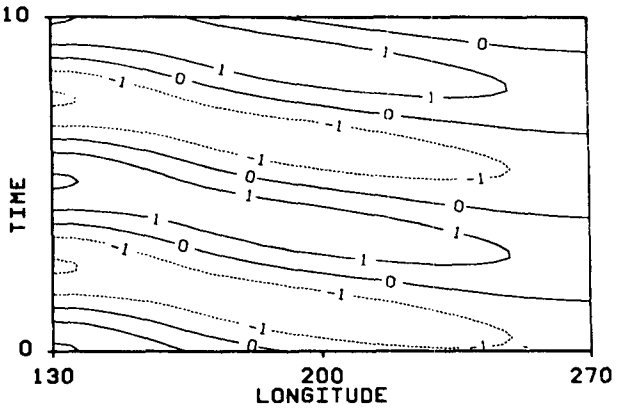

FIG. 8. Time–longitude dependence along the equator of the SST component of the westward-propagating SST mode with $\delta_s = 1.0$, $\mu = 0.1$.

5. Summary and discussion

Identifying and understanding the modes of the coupled tropical ocean–atmosphere system has been a key issue for our understanding of the dynamics of its interannual variability. Starting from the two ingredients that are familiar from the uncoupled problem—SST modes and the ocean basin modes—we demonstrated numerically in Part I how they merge in the coupled parameter space and argued that they are best thought of as *mixed SST/ocean-dynamics modes,* where "ocean dynamics" refers to the involvement of the time scales of subsurface dynamical processes. Here and in Part III, we present analytical or near-analytical results to provide physical insight into the coupled modes and an indication of the robustness of the numerical results.

In this part, we set up the basis for the analytical work, providing a scaling of the coupled system that singles out a few crucial parameters from a potentially large physical parameter space. We then give a formulation of the coupled eigenvalue problem in a finite basin, which is particularly useful for making approximations. An integral formulation for the response of the shallow-water ocean component for arbitrary temporal eigenvalue and zonal form of the spatial eigenvector is derived using results from Cane and Sarachik (1981) and Cane and Moore (1981). Combined with the equatorial-band SST equation of N91 and a Gill (1980) atmospheric model integral operator, this yields an integro–differential eigenvalue problem. Approximations made to this integral form have the advantage that the most difficult boundary conditions, involving oceanic wave propagation effects and the effects of the limited domain on the atmosphere, are automatically included.

We then begin the project of obtaining simplified results in various limits. In this part, we concentrate on the *weak-coupling limit* that is closest to the uncoupled system upon which intuition about the coupled system has hitherto been based. Part III presents results for cases with coupling of order unity or larger.

For sufficiently weak coupling, series solutions can be obtained, beginning with the uncoupled modes at zeroth order. These series solutions have a finite radius of convergence that encompasses a significant range of coupling values. In the case of the SST modes, the effects of coupling dominate the structure of the mode even at very weak coupling, when the eigenvalue correction is still small. The uncoupled SST modes are rather boring, being simply solutions of the heat equation. However, the effects of coupling dominate in basin-scale SST modes for coupling values larger than the horizontal heat diffusion coefficient, which is tiny. The SST modes are thus fundamentally coupled entities even when damping by surface fluxes is still stronger than instability tendencies.

Examination of solutions for the gravest SST mode in this case show that it tends to be stationary, with coupling providing a pure growth tendency, over a substantial range of parameters for sufficiently low values of the surface-layer parameter. The growth rate tendency is maximum in the fast-wave limit, but the qualitative characteristics of the mode are not strongly modified away from this limit. The 2-degeneracy marking the transition from stationary to westward-propagating SST modes for larger values of the surface-layer coefficient is found even for low coupling. For the stationary SST mode case, trapping of the mode in the eastern basin is noted over a wide range of the relative time scale coefficient. This will be further examined in Part III, using the fast-wave limit.

The uncoupled modes for the ocean dynamics component are the ocean basin modes of Cane and Moore (1981) and a class of scattering modes. From the numerical results of Part I, we know that the scattering modes undergo radical alterations before connecting

to the coupled modes of interest, so we focus on the modification of the lowest-frequency ocean-basin mode. The corresponding coupled mode retains its resemblance to the uncoupled version through a modest range of coupling, but rapidly takes on a mixed character as coupling is increased, producing lower frequency and positive growth rates. In Part I, this segment of the continuously connected eigensurface was one of the paths that led from low coupling to the important"standing oscillation" regime, that is, with standing oscillation in the SST components and with subsurface ocean dynamics providing the memory of the system. Even in the weak coupling limit, it may be seen that the structure of the mode takes on the characteristics of this mixed SST/ocean-dynamics mode.

Because we have a series solution valid for a significant range of coupling, we can roughly define the boundary between where this eigensurface can be thought of as a weakly coupled ocean basin mode and where it must be considered a fundamentally coupled mixed mode. It is clear from the form of the series solution that the time derivative of the SST equation formally enters the structure of the mode and the eigenvalue correction for all nonzero coupling values and becomes important as the correction terms begin to affect the structure of the mode, heralding the onset of "mixed-mode" characteristics. We evaluate the eigenvalue correction with and without taking the structural changes into account (corresponding to a zeroth- and high-order truncation of the series solution). The value of coupling at which the modification of the structure begins to have strong effects on the eigenvalue provides a good indication of where the mode becomes fundamentally mixed.

We conclude by suggesting that, in analyzing coupled models, terminology and intuition informed by the uncoupled case are likely to be of limited value when applied to modes of the coupled system. Even for relatively weak coupling, the coupled modes in a finite basin are unlike any uncoupled counterpart, especially in terms of their structure (this applies to the free modes of the system; it would be possible to obtain an uncoupled response resembling the coupled modes by using a wind forcing with spatial structure specified to resemble that of the coupled modes). For low-frequency, basin-scale variability, it is still less productive to attempt to decompose the modes in terms of the free Kelvin and Rossby modes of an infinite basin (unless the oceanic damping is unusually large). The uncoupled ocean-dynamics modes in a finite basin themselves bear little direct relation to individual Kelvin or Rossby modes, and the coupled modes contain large components that are associated with the coupled wind stress rather than with free wave propagation. We advocate that the more useful approach is to develop simple prototypes for the fully coupled modes and to understand how these connect to each other in the coupled parameter space. We pursue this avenue in Part III. The fast-wave limit, because of its simplicity, permits considerable insight into the growth mechanisms and into such important structural aspects as east basin trapping. We emphasize that the weak-coupling series solutions provided here are approximations to the same continuous eigensurface from a different part of the parameter plane. The series solution expanding from the gravest ocean basin mode at weak coupling provides one path of approximation to the "standing oscillation" regime. This path is useful for understanding some aspects of the dynamics, but in addition to suffering from rapid structural changes, it is not the only path from low coupling (as discussed in Part I). The growth and SST structure are best understood from the fast-wave limit stationary SST-mode solution discussed in Part III, which provides a more direct and unique path.

Acknowledgments. This work was supported in part by NSF Grants ATM-8905164 (JDN), ATM-9013217 (FFJ), and ATM-9215090 (FFJ and JDN). C. Wong provided invaluable assistance in typesetting the manuscript. It is a pleasure to acknowledge discussions with D. Battisti, P. Gent, J. McWilliams, G. Philander, E. Sarachik, and J. Tribbia. We thank M. Cane, who brought our attention to the "analytic ammunition" in CS81 and CM81, and M. Ghil, whose encouragement and support is much appreciated. An earlier version of part of this work appeared in the *Proceedings of the Eighth Conference on Atmospheric and Oceanic Waves and Stability,* American Meteorological Society, 1991.

APPENDIX A

Ocean Dynamics Spectrum

It has been shown by Moore (1968, chapter 4) that there exists a continuous spectrum of scattering modes in a linear shallow-water model of a zonally bounded ocean on an equatorial β plane. By "scattering modes," we simply mean free modes for which energy must be incident into the system, for example, equatorward along the western boundary, since leakage occurs poleward along the eastern boundaries. Cane and Moore (1981) further showed that under the long-wave approximation, a subset of this scattering spectrum (the least leaky modes) form quantized standing oscillatory ocean basin modes. In this appendix, we will show that under conventional representations of the long-wave approximation, in addition to the ocean basin modes, there are other quantized free modes, corresponding to the remainder of the scattering spectrum. We will refer to these modes as scattering modes since they are discretized versions of the leakier part of the scattering spectrum in the continuous case. These modes have not been noted in previous treatments. However, inclusion of these scattering modes is required for completeness of the system in terms of expressing initial conditions, etc.

From (3.9), the eigenvalue equation is obtained when the denominator of b_N vanishes. This yields

$$1 - \sum_{l=1}^{N} \frac{(2l-3)!!}{(2l)!!} z^l = 0$$

$$z = e^{-4\sigma}, \qquad \text{(A.1)}$$

where we denote $(2l)!! = 2\cdot 4\cdot 6\cdots 2l$, $(-1)!! \equiv 1$. For an oscillation of given frequency, the truncation N should be finite (see CS81) and given by the turning latitude, y_T, $2N + 1 = O(y_T^2)$. Thus, N becomes very large only for very low frequencies. Furthermore, the limits of integration on the western boundary condition (3.6) should also be given by the turning latitude. In solving for free modes with complex frequency, such treatment is nontrivial. Conventional numerical solutions use fixed truncation, and so we present the scattering modes for this case.

Letting z_n denote the nth root of the Nth-order polynomial (A.1), the eigenvalues are

$$-4\sigma_{n,k} = lnz_n - i2k\pi$$

$$n = 1, 2, \cdots, N$$

$$k = 0, 1, 2, \cdots, \qquad \text{(A.2)}$$

where k is the node number of the eigenfunction along the zonal direction. As N becomes large, the number of roots increases proportionally. Numerically, it appears that the z_n tend to converge to an almost evenly spaced distribution on a unit circle in the complex plane as shown in Fig. A1. The fact that all z_n lie outside the circle implies that the corresponding modes are decaying faster than the ocean damping rate ϵ_m. The decay rates decrease as N becomes large.

The single root whose decay rate is closest to the physical decay time is a real root with a value close to one. This is the root that corresponds to the ocean basin modes of Cane and Moore (1981). As $N \to \infty$, the root approaches one, that is, decays at exactly the physical decay time. To show this and to see why the ocean basin modes were more easily found than the remainder of the spectrum, consider that if $|z| \leq 1$, the sum in (3.5) would be convergent and (A.1) would become

$$(1 - z)^{1/2} = 0.$$

These assumptions, similar to those made in Gill (1985), CS81, and CM81, lead to a single solution, $z_1 \to 1$. In fact, all modes lie outside the radius for which the polynomial in (A.1) could be convergently summed for fixed z_n. The subtlety that $\{z_n\}$ change as a function of N is crucial to the convergence properties. This makes the remainder of the modes difficult to detect analytically. The eigenvalues related to the $z_1 = 1$ ocean basin mode root are

$$4\sigma = i2k\pi \quad k = 1, 2, \cdots. \qquad \text{(A.3)}$$

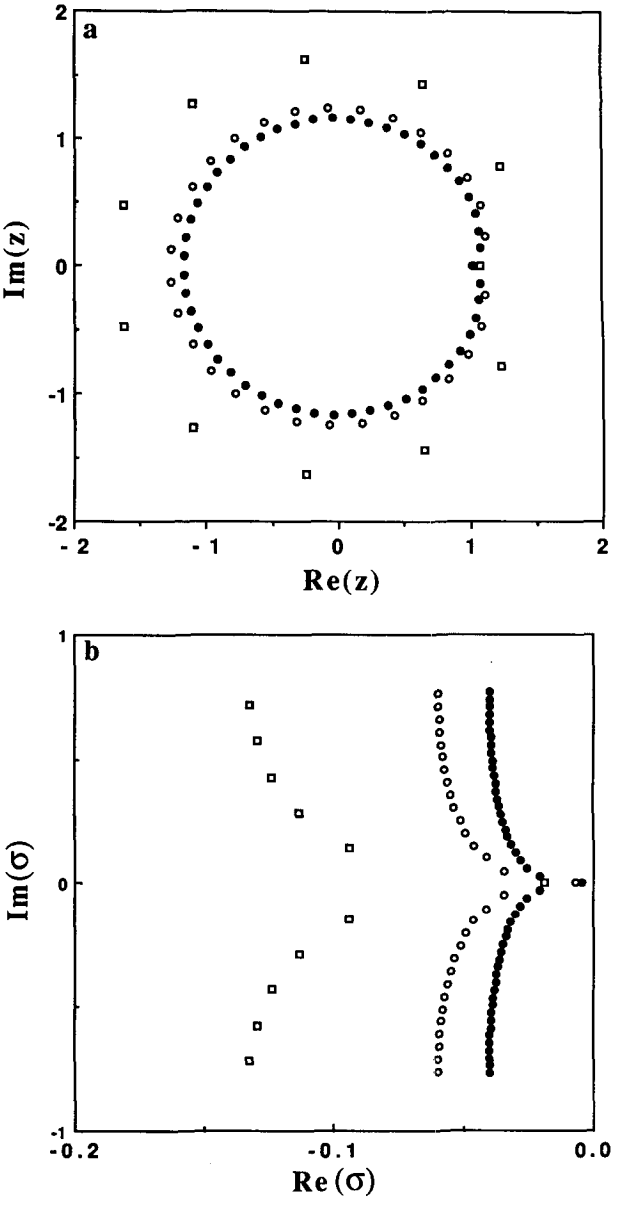

FIG. A1. Spectrum of uncoupled ocean modes (for the shallow-water equations in the long-wave approximation) for three different truncations: $N = 11$ (squares), $N = 31$ (circles), $N = 51$ (dots). (a) Roots $\{z_n\}$ of (A.4), (b) corresponding eigenvalues nondimensionalized by the Kelvin wave basin crossing time. The $k = 0$ set of (A.2) is shown; the pattern repeats along the frequency, Im(σ), axis with $k\pi/2$ added. Note that the Re(σ) axis is stretched so that decay rates can be more clearly seen.

The gravest ocean basin mode has the lowest frequency of $\sigma_1 = i\pi/2$, that is, a period four times the time taken by the Kelvin wave to cross the ocean basin. Its structure is characterized by change in the temporal phase of h at a node in the center of the basin, with the thermocline oscillation in the western part of the basin leading that in the eastern part and large u velocity in the center of the basin. Time–longitude plots of these

quantities are given in CM81. For the $z_1 = 1$ root and $k = 0$ in (A.3), one obtains the h = const, $u = 0$ solution. We note that this is not in fact a pole in (3.10); in other words, the h = const solution disappears under even tiny coupling. Numerical results in Part I show that it is absorbed by the SST mode (desingularization occurs through discretization—a diffusion term would also serve this function).

For $k = 0$ in (A.2), the other complex roots $\{z_n, n \neq 1\}$ give rise to modes of lower frequency, in the range of $(0, \pi/2)$. Different truncations will result in a slightly different distribution of the low-frequency modes. Since there are $(N-1)$ modes in this range, as $N \to \infty$, the frequency separation becomes correspondingly small. These modes thus provide the analog under the long-wave approximation to the continuous scattering spectrum of the full shallow-water equations. The "overdamping" in the sense that these modes decay faster than the physical decay rate simply corresponds to the fact that incident energy is required for a neutral scattering mode. The structures of symmetric scattering mode solutions are given by

$$q(x, y, t) = \sum_{l=1}^{N} q_{2l}(x, t)\psi_{2l}(y),$$

$$q_{2l}(x, t) = \tilde{q}_0\left(\frac{(2l-1)!!}{(2l)!!}\right)^{1/2} \times \exp\{\sigma[4l(x-1) - x + t] - \epsilon_m t\} \quad \text{(A.4)}$$

where $q = u + h$.

For related discretized systems with truncation N in the meridional and K degrees of freedom in the zonal direction, there are K ocean basin modes and $(N-1)K$ scattering modes, giving a complete eigenspectrum of KN modes. In any numerical model, the individual modes of the scattering spectrum will be sensitive to the model resolution. Indeed, we find such sensitivity in the model of section 2 of Part I both in the eigenvalues and eigenvectors at zero coupling, although ocean basin modes are less affected than the scattering spectrum because they approach well-defined frequencies. For the coupled problem reported in section 4 of Part I, sufficient zonal resolution for a given meridional truncation is important. The sensitivity of wave-related modes to resolution at weak coupling disappears for realistically strong coupling for the leading coupled modes.

The interaction of the scattering spectrum with wind forcing has not been explicitly studied but there are indications that interesting effects can arise. T. P. Barnett, M. Latif and collaborators (1993, personal communication) note that an ocean GCM stochastically forced by wind stress that is temporally white but spatially coherent with a large-scale structure comparable to interannual patterns can apparently produce a broad spectral peak at interannual time scales. It is possible that this is due to the wind structure projecting preferentially onto modes of the scattering spectrum in a particular frequency band. If this role of the scattering spectrum holds true, then the results of forcing an ocean model with noise that is also spatially white should be very different from using noise with coherent spatial structures, especially those similar in spatial pattern to interannual coupled variability.

APPENDIX B

Notation for Equatorial Wave Functions

The Fourier coefficients of the directly forced Kelvin and Rossby wave response to wind stress forcing of the form $\mathcal{A}_e\delta(x - x_0)Y(y)$, where $\delta(x - x_0)$ is the Dirac delta function, and $d_K e^{ikx_0}$ and $r_n e^{ikx_0}$, respectively, with

$$d_K = 2^{-1/2}(Y)_0$$

$$r_n = [(Y_y)_n - (2n+1)^{-1}(yY)_n]$$

where

$$(\ \ )_n = \int_{-\infty}^{\infty} (\ \ )\psi_n(y)dy,$$

$$\psi_n(y) = [\pi^{1/2}2^n n!]^{-1/2}H_n(y)\exp[-y^2/2]$$

and $H_n(y)$ are the Hermite polynomials.

Following Cane and Sarachik (1981), normalized Kelvin and Rossby vector functions are defined as

$$\mathbf{M}_K = 2^{-1/2}[\psi_0, \psi_0]^T$$

$$\mathbf{R}_n = \frac{1}{2\sqrt{2}}\begin{bmatrix}(n+1)^{-1/2}\psi_{n+1} - n^{-1/2}\psi_{n-1} \\ (n+1)^{-1/2}\psi_{n+1} + n^{-1/2}\psi_{n-1}\end{bmatrix}.$$

REFERENCES

Barnett, T. P., 1991: The interaction of multiple time scales in the tropical climate system. *J. Climate,* **4,** 269–285.

——, M. Latif, E. Kirk, and E. Roeckner, 1991: On ENSO physics. *J. Climate,* **4,** 487–515.

Battisti, D. S., 1988: The dynamics and thermodynamics of a warming event in a coupled tropical atmosphere/ocean model. *J. Atmos. Sci.,* **45,** 2889–2919.

——, and Hirst, A. C., 1989: Interannual variability in a tropical atmosphere–ocean model: Influence of the basic state, ocean geometry and nonlinearity. *J. Atmos. Sci.,* **46,** 1687–1712.

Bjerknes, J., 1969: Atmospheric teleconnections from the equatorial Pacific. *Mon. Wea. Rev.,* **97,** 163–172.

Cane, M., 1986: El Niño. *Ann. Rev. Earth Planet. Sci.,* **14,** 43–70.

——, and D. W. Moore, 1981: A note on low-frequency equatorial basin modes. *J. Phys. Oceanogr.,* **11,** 1578–1584.

——, and E. S. Sarachik, 1981: The response of a linear baroclinic equatorial ocean to periodic forcing. *J. Mar. Res.,* **39,** 651–693.

——, and S. E. Zebiak, 1985: A theory for El Niño and the Southern Oscillation. *Science,* **228,** 1084–1087.

——, M. Münnich, and S. E. Zebiak, 1990: A study of self-excited oscillations of the tropical ocean–atmosphere system. Part I: Linear analysis. *J. Atmos. Sci.,* **47,** 1562–1577.

Chao, Y., and S. G. H. Philander, 1993: On the structure of the Southern Oscillation. *J. Climate,* **6,** 450–469.

Deser, C., and J. M. Wallace, 1990: Large-scale atmospheric circulation features of warm and cold episodes in the tropical Pacific. *J. Climate,* **3,** 1254–1281.

Ghil, M., and R. Vautard, 1991: Interdecadal oscillations and the warming trend in global temperature time series. *Nature,* **350,** 324–327.

Gill, A. E., 1980: Some simple solutions for heat induced tropical circulation. *Quart. J. Roy. Meteor. Soc.,* **106,** 447–462.

——, 1985: Elements of coupled ocean–atmosphere models for the tropics. *Coupled Ocean–Atmosphere Models, Elsevier Oceanogr. Ser.,* 40, Elsevier, 303–328.

——, and E. M. Rasmusson, 1983: The 1982–1983 climate anomaly in the equatorial Pacific. *Nature,* **306,** 229–234.

Graham, N. E., and W. B. White, 1990: The role of the western boundary in the ENSO cycle: Experiments with coupled models. *J. Phys. Oceanogr.,* **20,** 1935–1948.

——, J. Michaelsen, and T. P. Barnett, 1987a: An investigation of the El Niño–Southern Oscillation cycle with statistical models. 1. Predictor field characteristics. *J. Geophys. Res.,* **92,** 14 251–14 270.

——, ——, and ——, 1987b: An investigation of the El Niño–Southern Oscillation cycle with statistical models. 2. Model results. *J. Geophys. Res.,* **92,** 14 271–14 289.

Hirst, A. C., 1988: Slow instabilities in tropical ocean basin–global atmosphere models. *J. Atmos. Sci.,* **45,** 830–852.

Jin, F.-F., and J. D. Neelin, 1993a: Modes of interannual tropical ocean–atmosphere interaction—a unified view. Part I: Numerical results. *J. Atmos. Sci.,* **50,** 3477–3503.

——, and ——, 1993b: Modes of interannual tropical ocean–atmosphere interaction—a unified view. Part III: Analytical results in fully coupled cases. *J. Atmos. Sci.,* **50,** 3523–3540.

Kuklinski, R., 1984: The effect of wind measurement errors on linear simulations of equatorial circulations. M. S. thesis, Department of Earth, Atmospheric and Planetary Sciences, Massachusetts Institute of Technology, 208 pp.

Lau, K. M., and P. J. Sheu, 1988: Annual cycle, quasi-biennial oscillation and southern oscillation in global precipitation. *J. Geophys. Res.,* **93,** 10 975–10 988.

Moore, D. W., 1968: Planetary-gravity waves in an equatorial ocean. Ph.D. thesis, Harvard University, 207 pp.

Münnich, M., M. A. Cane, and S. E. Zebiak, 1991: A study of self-excited oscillations in a tropical ocean–atmosphere system. Part II: Nonlinear cases. *J. Atmos. Sci.,* **48,** 1238–1248.

Neelin, J. D., 1990: A hybrid coupled general circulation model for El Niño studies. *J. Atmos. Sci.,* **47,** 674–693.

——, 1991: The slow sea surface temperature mode and the fast-wave limit: Analytic theory for tropical interannual oscillations and experiments in a hybrid coupled model. *J. Atmos. Sci.,* **48,** 584–606.

——, M. Latif, M. A. F. Allaart, M. A. Cane, U. Cubasch, W. L. Gates, P. R. Gent, M. Ghil, C. Gordon, N. C. Lau, C. R. Mechoso, G. A. Meehl, J. M. Oberhuber, S. G. H. Philander, P. S. Schopf, K. R. Sperber, T. Tokioka, J. Tribbia, and S. E. Zebiak, 1992: Tropical air–sea interaction in general circulation models. *Climate Dyn.,* **7,** 73–104.

Pan, Y.-H., and A. H. Oort, 1991: Correlation analyses between sea surface temperature anomalies in the eastern equatorial Pacific and the world ocean. *Climate Dyn.,* **4,** 191–205.

Philander, S. G. H., 1990: *El Niño, La Niña, and the Southern Oscillation.* Academic Press, 293 pp.

——, and R. C. Pacanowski, 1980: The generation of equatorial currents. *J. Geophys. Res.,* **85,** 1123–1136.

——, T. Yamagata, and R. C. Pacanowski, 1984: Unstable air–sea interactions in the tropics. *J. Atmos. Sci.,* **41,** 604–613.

Rasmusson, E. M., and T. H. Carpenter, 1982: Variations in tropical sea surface temperature and surface wind fields associated with the Southern Oscillation/El Niño. *Mon. Wea. Rev.,* **110,** 354–384.

——, and J. M. Wallace, 1983: Meteorological aspects of El Niño/Southern Oscillation. *Science,* **222,** 1195–1202.

——, X. Wang, and C. F. Ropelewski, 1990: The biennial component of ENSO variability. *J. Mar. Syst.,* **1,** 71–96.

Ropelewski, C. F., and M. S. Halpert, 1987: Global and regional scale precipitation associated with El Niño–Southern Oscillation. *Mon. Wea. Rev.,* **115,** 1606–1626.

Schopf, P. S., and M. J. Suarez, 1988: Vacillations in a coupled ocean–atmosphere model. *J. Atmos. Sci.,* **45,** 549–566.

——, and ——, 1990: Ocean wave dynamics and the time scale of ENSO. *J. Phys. Oceanogr.,* **20,** 629–645.

Wakata, Y., and E. S. Sarachik, 1991: Unstable coupled atmosphere–ocean basin modes in the presence of a spatially varying basic state. *J. Atmos. Sci.,* **48,** 2060–2077.

Wyrtki, K., 1975: El Niño—the dynamic responses of the equatorial Pacific ocean to atmospheric forcing. *J. Phys. Oceanogr.,* **5,** 572–584.

Zebiak, S. E., and M. A. Cane, 1987: A model El Niño Southern Oscillation. *Mon. Wea. Rev.,* **115,** 2262–2278.